(24) Zimm, B. H.; Bragg, J. K. *J. Chem. Phys.* **1959**, *31*, 526.
(25) von Dreele, P. H.; Poland, D.; Scheraga, H. A. *Macromolecules* **1971**, *4*, 396.
(26) Lin, T.-H.; Leed, A. R.; Scheraga, H. A.; Mattice, W. L. *Macromolecules* **1988**, *21*, 131.
(27) Igou, D. K.; Lo, J. T.; Clark, D. S.; Mattice, W. L.; Younathan, E. S. *Biochem. Biophys. Res. Commun.* **1984**, *23*, 1595.
(28) Overgaard, T.; Erie, D.; Darsey, J. A.; Mattice, W. L. *Biopolymers* **1984**, *23*, 1595.
(29) Dygert, M. K.; Taylor, G. T.; Cardinaux, F.; Scheraga, H. A. *Macromolecules* **1976**, *9*, 794.
(30) Lakowicz, J. R. *Principles of Fluorescence Spectroscopy*; Plenum: New York, 1983; p 131.
(31) Mukerjee, P.; Mysels, K. J. *Critical Micelle Concentrations of Aqueous Surfactant Solutions*; National Bureau of Standards, NSRDS-NBSs36; U.S. Government Printing Office: Washington, DC, 1971.
(32) Mattice, W. L.; Lo, J. T.; Mandelkern, L. *Macromolecules* **1972**, *5*, 729.
(33) von Dreele, P. V.; Lotan, N.; Ananthanarayanan, V. S.; Andreatta, R. H.; Poland, D.; Scheraga, H. A. *Macromolecules* **1971**, *4*, 408.
(34) Lin, T.-H.; Cherry, W. R.; Mattice, W. L. *Polym. Commun.* **1986**, *27*, 37.
(35) McCord, R. W.; Blakeney, E. W.; Mattice, W. L. *Biopolymers* **1977**, *16*, 1319.

Configurational Properties of Finite Cyclic Alkanes

Wayne L. Mattice*

Department of Polymer Science, The University of Akron, Akron, Ohio 44325

Robert G. Snyder

Department of Chemistry, University of California, Berkeley, California 94720.
Received December 8, 1987

ABSTRACT: The dependence of local chain configurations on the number of bonds, n, has been examined for cyclic alkanes. Discrete enumeration is used for identification of all nonintersecting rings with $6 \le n \le 22$ on a tetrahedral lattice. Rotational isomeric state theory provides the information for infinitely large rings. Interpolations suggest the behavior of rings of intermediate size, $22 < n < \infty$. Ensembles are weighted in various ways, including (1) all rings weighted equally; (2) $\sigma = 0.43$, which incorporates the butane effect; and (3) $\sigma = 0.43$ and $\omega = 0.034$, which incorporates both the butane and pentane effects. Probabilities are evaluated for occupation of all rotational isomers and for all pairs of rotational isomers at successive bonds. The dominant ring configurations at $6 \le n \le 22$ are identified.

Introduction

The configurational characteristics of cyclic alkanes undergo drastic changes as the number of bonds, n, increases from six to infinity. This conclusion follows immediately from the observation that the cyclic chain with $n = 6$ does not have any bond in a trans state, but the majority of the bonds occupy trans states as n becomes infinite. The occupancy of rotational states in infinitely large cyclic polyethylenes is easily calculated from the known behavior of large linear polyethylene chains.[1,2] The calculation presents a more difficult problem for rings that contain 10–100 bonds. Nevertheless, the results for chains of 10–100 bonds are of interest because it is here that the bulk of the transition from cyclohexane to an infinitely large cyclic polyethylene takes place. This transition range is important for several reasons, including its use for deducing the configurational origin of various spectroscopic transitions observed in cyclic alkanes. The diamond lattice rings described here will be used in the analysis of the vibrational spectra of cycloalkanes $C_{14}H_{28}$, $C_{16}H_{32}$, and $C_{22}H_{44}$.[3] Calculations have been performed for cyclic polyethylenes with even n, $6 \le n \le 22$. These calculations cover a range that adequately defines an extrapolation to the known limits for infinitely large rings. Therefore, the motivation for this work is somewhat different from the driving force in previous studies of the dimensions of unperturbed[4] and perturbed[5–7] rings, probability for ring closure,[8,9] or rate of intramolecular cyclization.[10–12] The motivation is more closely related to the description of the local configurations that are consistent with ring closure.[13–17]

Methods

All possible configurations were examined for linear chains that are confined to a tetrahedral lattice and have an even number of bonds in the range 6–22. Average properties were computed for those chains that have an end-to-end distance of zero but do not otherwise intersect. This averaging was achieved using several different values of σ and ω, which are the statistical weights for first- and second-order interactions in the rotational isomeric state model developed for linear polyethylene by Abe et al.[7] These combinations of statistical weights are presented in Table I. The first pair of statistical weights considers all configurations to be of equal energy, the second pair penalizes gauche states in the manner expected for polyethylene at 300 K, and the third combination also invokes the penalty for the "pentane effect" in the manner expected at that temperature. The fourth, fifth, and sixth combinations invoke the butane and pentane effects in the manner expected at temperatures of 350, 400, and 450 K, respectively.

Table I
Combinations of Statistical Weights Used

σ	ω	comment
1.000	1.000	configurations equally weighted
0.432	1.000	butane effect, 300 K
0.432	0.034	butane and pentane effects, 300 K
0.487	0.056	butane and pentane effects, 350 K
0.533	0.081	butane and pentane effects, 400 K
0.572	0.106	butane and pentane effects, 450 K

Averages of configuration-dependent properties for unperturbed linear chains were evaluated by using standard matrix methods.[1,2,18]

Results and Discussion

Occurrence of Nonintersecting Cyclic Chains. The configuration partition function for the unperturbed chain is denoted by Z[1,2] and is calculated as

$$Z = \{(1 - \lambda_2)\lambda_1^{(n-1)} + (\lambda_1 - 1)\lambda_2^{(n-1)}\}/(\lambda_1 - \lambda_2) \quad (1)$$

$$\lambda_1, \lambda_2 = \{1 + \sigma + \sigma\omega \pm [(1 - \sigma - \sigma\omega)^2 + 8\sigma]^{1/2}\}/2 \quad (2)$$

where λ_1 and λ_2 are the eigenvalues of the statistical weight

0024-9297/88/2221-2452$01.50/0

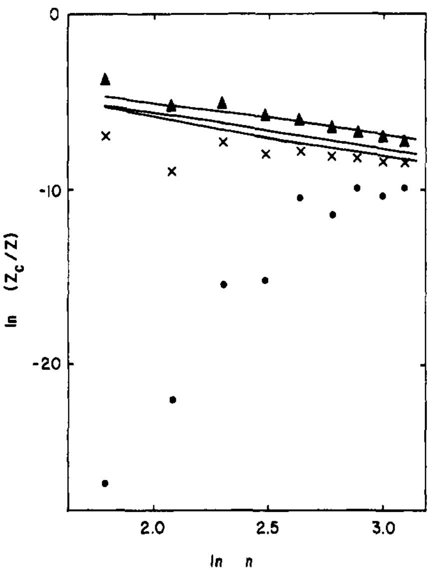

Figure 1. Solid lines depict Z_c/Z when it is approximated by eq 3. The points depict Z_c/Z when Z_c and Z are obtained from the tetrahedral lattice and eq 1, respectively. The sets of statistical weights are $\sigma = \omega = 1$ (top line and triangles), $\sigma = 0.432$ and $\omega = 1$ (middle line and ×'s), and $\sigma = 0.432$ and $\omega = 0.034$ (bottom line and filled circles).

matrix, with $\lambda_1 > \lambda_2$.[1] A smaller configuration partition function, denoted by Z_c, describes the chains that have an end-to-end distance of zero but do not otherwise intersect. This latter partition function is obtained from the examination of the chains grown on a tetrahedral lattice.

The solid lines in Figure 1 are obtained with the first three sets of statistical weights in Table I and the approximation

$$Z_c/Z = [3/2\pi\langle r^2\rangle_0]^{3/2} \tag{3}$$

where $\langle r^2\rangle_0$ is the mean square unperturbed end-to-end distance of the linear chain. Equation 3 gives the probability for cyclization of a long random flight chain.[8,9] This equation should serve as an excellent approximation to the true Z_c/Z for sufficiently large unperturbed chains. Equation 3 provides a fairly good description of chains with n of 10–22 if all configurations are weighted equally. When there is discrimination against gauche states, eq 3 provides an overestimate of Z_c/Z, but it approximates the trend for chains with n = 12–22. Equation 3 predicts neither the size of Z_c/Z nor the dependency of Z_c/Z upon n, when $\sigma = 0.43$, $\omega = 0.034$, and n is 6–22. In this case, Z_c/Z initially increases with n and appears to reach a maximum at n near 22, which is the largest n studied. There must indeed be a maximum because Z_c/Z must decrease with n as the number of bonds becomes infinite. The fact that this trend is seen in Figure 1 when $\sigma = \omega = 1$, but is absent when $\sigma = 0.432$ and $\omega = 0.034$, shows that realistic weighting of the rotational isomers in polyethylene has a profound influence on the properties of rings with 6–22 bonds. The penalty associated with consecutive gauche placements of opposite sign, which is denoted by ω, plays a particularly important role in the values of Z_c/Z for small rings.

First-Order Probabilities. Figure 2 depicts the probability for a trans placement as a function of $1/n$. The limit at infinitely large n must be identical for rings and linear chains. This limit is $1/(1 + 2\sigma)$ if $\omega = 1$ because the bonds are then independent. The limit can be computed by matrix methods if the bond rotations are interdependent, i.e., if ω is different from 1. When $\sigma = 0.432$ and $\omega = 0.034$, the limit is 0.64. In view of the symmetry of the rotation about internal bonds in polyethylene, the probabilities for either of the two gauche states at any n are $(1 - p(t))/2$.

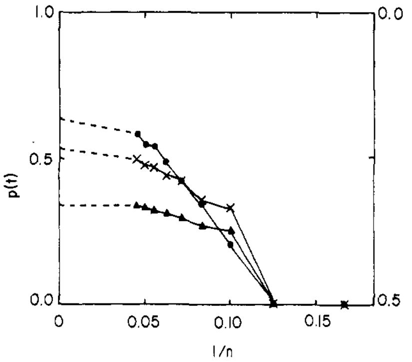

Figure 2. Probability for a trans placement in the cyclic chains as a function of $1/n$. The sets of statistical weights are the same as those used for the symbols plotted in Figure 1.

Table II
Cyclic Chains with $n = 10$[a]

configuration	g	exponents for σ	exponents for ω	$p(t)$
0++−+0++−+	20	8	4	0.2
00+−+00+−+	10	6	4	0.4
++0++−−0−−	10	8	2	0.2

[a] Configurations are denoted by 0 = trans, + = gauche +, − = gauche −. Representation of the conformation of a cyclic alkane by a linear string requires arbitrary decisions on the bond at which the sequence starts and whether indexing of the bonds proceeds in a clockwise or counterclockwise manner. Each of the $2n$ linear strings has a mirror image obtained by interconversion of all "+" and "−". The degeneracy, g, is the number of nonidentical strings. The upper limit for g is $4n$.

The value of $p(t)$ is 0.331 at $n = 20$ when all configurations are weighted equally. This value is nearly identical with the expected limit of 1/3 at infinite n. Smaller rings have a lower content of trans placements, and trans placements are completely absent in rings of six and eight bonds. When gauche states are penalized with $\sigma = 0.432$, the probability of a trans state rises to 0.536 in the infinite chain, but it is only 0.498 at $n = 22$. The approach to the limit is delayed when σ is less than one. There is a slightly greater delay if ω is assigned the value expected in polyethylene at 300 K. When $\sigma = 0.432$ and $\omega = 0.034$, the limiting $p(t)$ is 0.64, but the value at $n = 22$ is only 0.584. The fraction of the bonds with trans placements in the rings with $n = 22$ is 93% of that of an infinite ring if $\sigma = 0.432$ and $\omega = 1$, and this value becomes 91% if $\sigma = 0.432$ and $\omega = 0.034$.

The $p(t)$ for rings in which $n > 22$ can be estimated by linear extrapolation from the point for the ring with $n = 22$ to the known limit at $1/n = 0$. This extrapolation is depicted as a dashed line in Figure 2.

The ring with $n = 10$ exhibits $p(t)$ that do not conform to the naive expectation that $p(t)$ should increase upon a decrease in σ or ω. The origin of the observed $p(t)$ at $n = 10$ becomes apparent upon enumeration of all 40 rings. These configurations are listed in Table II. A simple calculation shows that $p(t)$ is 0.25 if all chains are weighted equally. The second entry in Table II becomes dominant as σ decreases while ω is held at one. As σ becomes vanishingly small, $p(t)$ must approach 0.4. However, if it is ω that becomes vanishingly small, then it is at the last entry in Table II that is dominant, and $p(t)$ will approach 0.2.

Second-Order Probabilities. All of the second-order probabilities are depicted in Figure 3. The limiting values

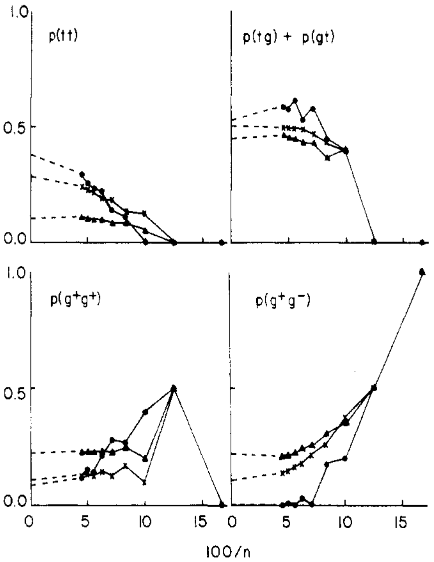

Figure 3. Second-order probabilities for the cyclic chains. The bond pairs are trans–trans in the upper left, trans–gauche (in any order and of any sign) in the upper right, gauche placements of the same sign in the lower left, and gauche placements of opposite sign in the lower right. The sets of statistical weights are the same as those used for the symbols plotter in Figure 1.

at finite n are least sensitive to the three choices of statistical weight assignments when the bond pair is trans–gauche. When there are two gauche placements of the same sign, the limit is sensitive to the change in σ but rather insensitive to the change in ω. Of course, the value of ω is extremely important when the two gauche placements are of opposite sign.

In all four panels, the ring with $n = 22$ has second-order probabilities that are very close to those expected for an infinite ring when all configurations are weighted equally. The values (with the infinite ring in parenthesis) are $p(\mathrm{tt}) = 0.109$ (0.111), $p(\mathrm{tg}) = 0.458$ (0.444), $p(\mathrm{g^+g^+}) = 0.229$ (0.222), and $p(\mathrm{g^+g^-}) = 0.206$ (0.222).

When $\sigma = 0.432$ and $\omega = 1$, the ring with $n = 22$ has $p(\mathrm{tg}) = 0.496$, which is nearly identical with the limiting value of 0.500. The ring with $n = 22$ has an excess of gauche pairs, and a reduction of trans pairs, when compared with the infinite ring. There is an oscillation in $p(\mathrm{g^+g^+})$. This oscillation must also occur in the sum of all of the other second-order probabilities. However, that oscillation in the individual $p(\mathrm{tt})$, $p(\mathrm{tg})$, and $p(\mathrm{g^+g^+}-)$ is masked in Figure 3 because these three second-order probabilities are more strongly dependent on n, in the region where $10 \leq n \leq 20$, than is $p(\mathrm{g^+g^+})$.

If $\sigma = 0.432$ and $\omega = 0.034$, the best agreement between $n = 22$ and $n = \infty$ is seen in the nearly complete suppression of gauche pairs of opposite sign. The ring with $n = 22$ how has an excess of trans–gauche pairs and gauche pairs of the same sign. There is a large deficiency in trans pairs. The second-order a priori probabilities for larger rings can be estimated by the linear extrapolation to the known limits in Figure 3. This extrapolation suggests that the deficiency in trans pairs, and the excess of tg and $\mathrm{g^+g^+}$ pairs, should persist to n significantly larger than 22. The ring must contain about 50 bonds before $p(\mathrm{tt})$ comes with 10% of the value for an infinitely large ring.

Figure 4 depicts selected ratios of the second-order probabilities. These ratios are of interest because experimental values are accessible from the ratios of the intensities of selected vibrational bands.[3] The reference state is the probability for a pair of trans states. The smallest ring considered in Figure 4 has $n = 10$ because the rings with $n = 6$ and 8 contain no trans placements. The left portion of the figure shows the ratio of all other second-order probabilities to $p(\mathrm{tt})$. In the middle and right-hand portions, the result at the left is broken down into contributions from tg (middle) and gg (right).

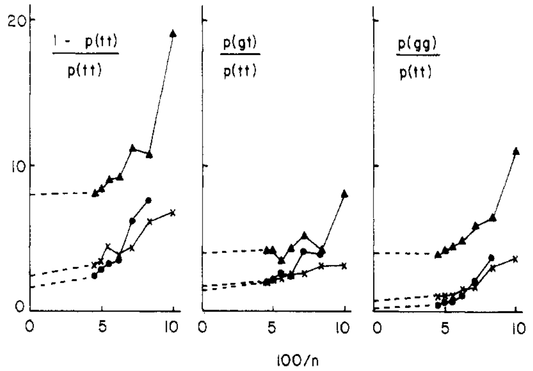

Figure 4. Selected ratios of the second-order probabilities. The sets of statistical weights are the same as those used for the symbols plotted in Figure 1.

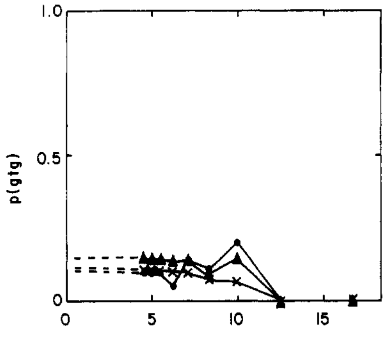

Figure 5. Probability of gtg triplets. The gauche placements may be of either sign. The sets of statistical weights are the same as those used for the symbols plotted in Figure 1.

The limits for the infinite rings are all markedly reduced when σ decreases from 1 to 0.432. A further reduction takes place upon the decrease of ω from 1 to 0.034, with this additional reduction being most dramatic in the right panel and least dramatic in the middle panel.

All of the ratios approach their limiting values from above because $p(\mathrm{tt})$ is suppressed in rings of finite n. At $n = 22$, the equally weighted rings have ratios that are in excellent agreement with the limits for infinite rings, as expected from Figure 3. At this same n, the ratios exceed the infinite ring limits when the other two weighting schemes are employed.

A Selected Third-Order Probability. A third-order probability of particular interest is that for a trans placement flanked by gauche placements. The computed values are depicted in Figure 5. When all rings are weighted equally, the value is 0.149 at $n = 22$ and 0.148 in the infinite ring. Quite good agreement between $n = 22$ and $n = \infty$ is also obtained with the other two sets of statistical weights. In the case where $\sigma = 0.432$ and $\omega = 0.034$, there are rather broad oscillations in $p(\mathrm{gtg})$ for $n = 8$–18. The most important contribution to $p(\mathrm{gtg})$ is made by triplets in which both gauche placements are of the same sign, as is apparent upon inspection of Table III.

Dominant Configurations. Dominant configurations for the rings are collected in Table III. There is only a single distinct configuration at $n = 6$ and 8. The one configuration listed in Table III for $n = 10$ completely dominates the ensemble. (The other ring configurations

Table III
Dominant Configurations[a]

			exponents for		population at T			
n	configuration	g	σ	ω	300 K	350 K	400 K	450 K
6	+-+-+-	2	6	6	1.00	1.00	1.00	1.00
8	++--++--	4	8	4	1.00	1.00	1.00	1.00
10	0++--0++--	10	8	2	0.99	0.98	0.97	0.95
12	0-++0++0++-0	24	8	2	0.63	0.61	0.59	0.57
	00++--00++--	12	8	2	0.31	0.30	0.30	0.29
	00+-00+-00+-	8	6	3	0.04	0.05	0.06	0.06
	0+--0-+0++-0	24	8	3	0.02	0.03	0.05	0.06
14	0++0++00--0--0	14	8	0	0.93	0.87	0.80	0.72
	00++0++0+++0+-	56	9	1	0.05	0.09	0.14	0.17
	00+00-+00-00+-	14	6	2	0.01	0.01	0.02	0.02
16	0++00--00++00--0	8	8	0	0.56	0.41	0.30	0.23
	000++-00-00++0++	64	8	1	0.15	0.18	0.19	0.19
	+00+0++00--0-00-	32	8	1	0.08	0.09	0.10	0.10
	00+0++0+++0+00-+	64	9	1	0.07	0.09	0.10	0.11
	00-00+--0+0++0++	64	9	1	0.07	0.09	0.10	0.11
18	00+00+0++00-00-0--	36	8	0	0.17	0.16	0.14	0.12
	0+0++00-00+00--0-0	36	8	0	0.17	0.16	0.14	0.12
	0+00-00+00-00+00-0	6	6	0	0.15	0.11	0.08	0.06
	00+0+++0+00+0++00-	72	9	0	0.15	0.15	0.15	0.14
	00++0++0000--0--00	18	8	0	0.08	0.08	0.07	0.06
	0++000++00--000--0	18	8	0	0.08	0.08	0.07	0.06
	000++0+++0-0--00++	72	10	0	0.06	0.07	0.08	0.08
20	+000++00-00-00++000+	40	8	0	0.11	0.08	0.06	0.05
	++000++0+00++0+00-00	80	9	0	0.09	0.08	0.07	0.06
	+0+++000++0+00+00-00	80	9	0	0.09	0.08	0.07	0.06
	+00+0++0+0--00+00-00	80	9	0	0.09	0.08	0.07	0.06
	00++00--0000++00--00	20	8	0	0.05	0.04	0.03	0.03
	00++0+00+00-00-0--00	20	8	0	0.05	0.04	0.03	0.03
	00++00---0+0++00-00-	80	10	0	0.04	0.04	0.04	0.03
	00++00---0-00++0+00-	80	10	0	0.04	0.04	0.04	0.03
	00++0+0---0-00-00++0	80	10	0	0.04	0.04	0.04	0.03
	00++0+++0-00++00--00	80	10	0	0.04	0.04	0.04	0.03
22	00+00-00+0000-00+00-00	22	6	0	0.08	0.05	0.03	0.02
	00+00-00+00+0+00-0--00	88	8	0	0.06	0.04	0.03	0.03
	00+00+0++0000-00-0--00	44	8	0	0.03	0.02	0.02	0.01
	00+0++00-0000+00--0-00	44	8	0	0.03	0.02	0.02	0.01
	0++0+0000+00--0-0000-0	44	8	0	0.03	0.02	0.02	0.01
	00++00-00-00+00+00--00	44	8	0	0.03	0.02	0.02	0.01
	0++000+00+00--000-00-0	44	8	0	0.03	0.02	0.02	0.01
	0+00--000-00+00--000-0	44	8	0	0.03	0.02	0.02	0.01
	0+00+0+00+00-00-0-00-0	44	8	0	0.03	0.02	0.02	0.01

[a] Configurations listed account for the following fractions of Z_c at 300 K: $n = 10$, 0.99; $n = 12$, 1.00; $n = 14$, 0.99; $n = 16$, 0.92; $n = 18$, 0.87; $n = 20$, 0.66; $n = 22$, 0.32.

at $n = 10$ are listed in Table II.) There are two major configurations at $n = 12$, but a single configuration is dominant at $n = 14$. The chain with $n = 14$ is the smallest molecule that can achieve ring closure without recourse to the "pentane effect". This configuration of the ring therefore dominates the ensemble because ω does not occur in its statistical weight. At $n = 16$, there is also only one configuration that achieves ring closure without encountering the pentane effect, and that configuration accounts for over half of the configuration partition function of the ensemble at 300 K. Larger rings have several different ways of achieving ring closure without the pentane effect. For this reason, no single configuration is dominant when n is 18 or larger.

Temperature Dependence. Table III presents the temperature dependence of the populations of the major configurations. The most interesting temperature dependences are seen in the rings with 14 and 16 bonds. The first entries for these rings account for 93% and 56%, respectively, of the configuration partition functions at 300 K. These configurations dominate all others at low temperatures because the absence of a factor of ω gives them the largest statistical weights. However, as temperature increases, there is an increasingly vigorous competition by the larger number of configurations with ω in their statistical weights. Therefore the population of the dominant configuration is sensitive to temperature over the range 300–450 K when n is 14 or 16.

Acknowledgment. This research was supported by National Science Foundation Grant DMR 86-96071 (W. L.M.) and DMR 87-01586 (R.S).

References and Notes

(1) Flory, P. J. *Statistical Mechanics of Chain Molecules*; Wiley: New York, 1969; pp 72–73.
(2) Flory, P. J. *Macromolecules* **1974**, *7*, 381–392.
(3) Shannon, V. L.; Strauss, H. L.; Snyder, R. G.; Elliger, C. A.; Mattice, W. L., submitted for publication in *J. Am. Chem. Soc.*
(4) Zimm, B. H.; Stockmayer, W. H. *J. Chem. Phys.* **1949**, *17*, 1301–1314.
(5) Bruns, W.; Naghizadeh, J. *J. Chem. Phys.* **1976**, *65*, 747–751.
(6) Chen, Y. *J. Chem. Phys.* **1981**, *74*, 2034–2038.
(7) Baumgartner, A. *J. Chem. Phys.* **1982**, *76*, 4275–4280.
(8) Jacobson, H.; Stockmayer, W. H. *J. Chem. Phys.* **1950**, *18*, 1600–1606.
(9) Flory, P. J.; Suter, U. W.; Mutter, M. *J. Am. Chem. Soc.* **1976**, *98*, 5733–5739.
(10) Nairn, J. A.; Braun, C. L. *J. Chem. Phys.* **1981**, *74*, 2441–2449.
(11) Fraser, S. J.; Winnik, M. A. *J. Chem. Phys.* **1981**, *75*, 4683–4695.
(12) Noolandi, J.; Hong, K. M.; Bernard, D. A. *Macromolecules* **1984**, *17*, 2895–2901.
(13) Smith, R. P. *J. Chem. Phys.* **1965**, *42*, 1162–1166.
(14) Go, N.; Scheraga, H. A. *Macromolecules* **1970**, *3*, 178–187.

(15) Uiterwijk, J. W. H. M.; Harkema, S.; van de Waal, B. W.; Gobel, F.; Nibbeling, H. T. M. *J. Chem. Soc., Perkin Trans. 2* **1983**, 1843–1855.
(16) Bruccoleri, R. E.; Karplus, M. *Macromolecules* **1985**, *18*, 2767–2773.
(17) Saunders, M. *J. Am. Chem. Soc.* **1987**, *109*, 3150–3152.
(18) Abe, A.; Jernigan, R. L.; Flory, P. J. *J. Am. Chem. Soc.* **1966**, *88*, 631–639.

Excited Triplet State of Carbazole Chromophore and the Triplet Energy Migration in Poly[(carbazolylethyl methacrylate)-*co*-(methyl methacrylate)] Film

Shinzaburo Ito,* Hideaki Katayama, and Masahide Yamamoto*

Department of Polymer Chemistry, Faculty of Engineering, Kyoto University, Sakyo-ku, Kyoto 606, Japan. *Received December 2, 1987*

ABSTRACT: Triplet excimer formation and energy migration among carbazole chromophores in poly[(carbazolylethyl methacrylate)-*co*-(methyl methacrylate)] film were investigated by measuring phosphorescence. The use of the copolymer gave a polymer matrix with a high chromophore concentration but with uniform distribution of the carbazole moiety. Three triplet species were observed depending on the concentration of chromophore: monomer ($^3M^*$), shallow trap ($^3T^*$), and triplet excimer ($^3E^*$). Triplet energy migration occurs at concentrations higher than 0.9 mol L^{-1}, where the average distance of chromophore is about 1.2 nm. This energy transport brings a drastic change in the spectra from $^3M^*$ to $^3E^*$. Pulsed excitation gave a clear rise of sensitized phosphorescence from a triplet energy acceptor, 1,4-dibromonaphthalene. The diffusion coefficient of triplet energy (D) was found to be on the order of 10^{-9} cm^2 s^{-1} by evaluation from the rise time. Concentration dependence of D indicated that the energy hopping takes place with the electron-exchange mechanism.

Introduction

Photophysical processes of the carbazole chromophore have been the center of much attention from the fundamental as well as the application standpoint. Many workers have investigated the electronically excited states and their dissipation processes in poly(vinylcarbazole) and its dimeric model compounds.[1-10] In the triplet state as well as in the singlet state, the carbazole chromophore is said to form the excimer that is an excited dimer between an excited chromophore and a ground-state one.[11]

Compared with the singlet state, the knowledge on the triplet state is poor, because of the weak phosphorescence emission from the triplet state. But a large part of the excited energy dissipates to the ground state via the triplet state, and the fraction often exceeds a half of the excited chromophores. Thus, the triplet state is important when discussing the photofunctional properties of polymer solids.

Triplet-state behavior of many aromatic molecules besides the carbazole chromophore has been studied, e.g., naphthalene and phenanthrene.[12-14] The data obtained on these polymer systems indicate that there are two critical factors deciding the behavior of excited states in polymers, where the chromophores are fixed in a matrix at an extremely high concentration.[15-22] The first factor is trap-site formation. In a glassy solvent, the phosphorescence spectra from polymers often shift to the red side about a few nanometers; it is said to be a shallow trap formed between two neighboring chromophores on the polymer chain. Some polymer films show broad and red-shifted spectra, which are much like the fluorescence spectra of a singlet excimer. This was assigned to a triplet excimer, which acts as a deep trap of triplet energy. The second factor is migration of triplet energy. By triplet energy migration, an efficient energy flow occurs from donor molecules to a small amount of acceptor molecules or trap sites, which is called "sensitization". These two primary factors should be understood when discussing the photophysical processes in polymer systems.

After the detailed studies by Klöpffer et al.,[11] poly(vinylcarbazole) and its analogous polymers were widely investigated by using the time-resolved spectroscopic technique.[23-26] Especially, Burkhart et al. showed the existence of several triplet species in poly(vinylcarbazole) film and studied their behavior in a wide range of temperature.[23] Another effective approach has been carried out by modifying the chemical structure of polymers whose pendant chromophores were linked to the polymer chain in a form so as not to satisfy Hirayama's $n = 3$ rule.[27-30] These polymer structures weaken the interaction between chromophores and make the excited species simpler than those of poly(vinylcarbazole).

Copolymerized samples containing various amounts of the chromophoric monomer in a spectroscopically inert comonomer give another variation for the study of photophysics in polymer systems. Concentration dependence is an important factor to be scrutinized for the excimer formation and energy transfer processes. Both the phenomena result from the interaction of chromophores, that is, they are mainly governed by the distance of separation. However, in polymeric systems, homopolymers impose a fixed and vague local concentration. By the use of a series of copolymers prepared from a similar kind of methacrylate monomer, we can observe the nature of triplet states in the polymer solid as a function of the chromophore concentration. The investigation in this system will give an insight into the triplet state behavior in a wide range from an isolated chromophore to the highly concentrated systems where many interchromophoric processes take place.

Experimental Section

Materials and Sample Preparation. The monomer, 2-(9-carbazolyl)ethyl methacrylate (CzEMA), was synthesized by es-

0024-9297/88/2221-2456$01.50/0